Optimal Dynamical Gauge in the Quantum Rabi Model

Yuqi Qing[1], Liangsheng Li[2], Wen-Long You[3*], Yueheng Lan[1*], and Maoxin Liu[4*]

[1]*State Key Laboratory of Information Photonics and Optical Communications, Beijing University of Posts and Telecommunications, Beijing 100876, China*
[2]*Science and Technology on Electromagnetic Scattering Laboratory, Beijing 100854, China*
[3]*College of Science, Nanjing University of Aeronautics and Astronautics, Nanjing, 211106, China*
[4]*School of Systems Science/Institute of Nonequilibrium Systems, Beijing Normal University, Beijing 100875, China*

(Received 17 December 2024; accepted manuscript online 21 January 2025)

We have investigated the gauge dependence of physical observables in a quantum Rabi model under different potential fields arising from the Hilbert space truncation of the atomic degrees of freedom. In both the square-well and harmonic potentials, the optimal gauge for the ground-state energy depends on the cavity frequency, which is optimal in the low-frequency limit, whereas the Coulomb gauge is optimal in the high-frequency limit. For a dynamic quantity, such as an out-of-time-order correlator, we have demonstrated the necessity of introducing an optimal dynamic gauge. This study provides deeper insight into the intricate relationship between gauge choice and the dynamics of quantum electrodynamics systems, resulting in more accurate theoretical frameworks.

DOI: 10.1088/0256-307X/42/2/020501 CSTR: 32039.14.0256-307X.42.2.020501

Introduction. Gauge invariance is the cornerstone of modern physics. In classical electromagnetism, observables, such as the electric field $\boldsymbol{E}$ and the magnetic induction field $\boldsymbol{B}$ remain unchanged under gauge transformations. This principle extends to the gauge field theory, which forms the foundation of the standard model.[1] In non-relativistic quantum electrodynamics (QED), the $\boldsymbol{p}\cdot\boldsymbol{A}$ interaction in the Coulomb gauge is equivalent to the $\boldsymbol{r}\cdot\boldsymbol{E}$ interaction in the dipole gauge,[2] established via the Goppert–Mayer transformation.[3] However, in certain scenarios, gauge choices can yield different physical results or even non-physical predictions, a phenomenon known as gauge dependence. Lamb's study on the fine structure of hydrogen[4] showed that the probability amplitudes were correctly interpreted only in the dipole gauge. Singularities in the Coulomb gauge can be resolved by applying the Power–Zienau–Woolley transformation to a multipolar gauge.[5,6] Gauge dependence remains a persistent challenge that has been extensively studied in various contexts.[7–14]

In the context of light-matter interactions, the quantum Rabi model (QRM) has long served as a paradigmatic framework for describing the interaction between a two-level atom and an optical cavity field.[15,16] Recent advances have enabled the realization of strong coupling, ultra-strong coupling (USC), and deep strong coupling (DSC) regimes,[17–23] which have triggered renewed interest in QRM-based studies. These investigations encompass a wide range of phenomena, including coupling-induced effects,[24,25] nonlinear optics,[26] relaxation dynamics,[27] the use of QRM as the building blocks of superconducting circuits,[28–32] superradiant phase transitions,[33–41] and quantum integrability.[42–45]

Because of the two-level truncation applied to the atomic Hilbert space in deriving the Hamiltonian, the QRM is gauge dependent.[46,47] This dependence is more pronounced in the USC and DSC regimes.[46] Although the two-level approximation in the dipole gauge remains valid when specific potentials are selected, the Coulomb gauge fails in the USC regime. The Jaynes–Cummings (JC) model can be derived directly from the full Hamiltonian using the JC gauge, without requiring a rotating wave approximation, and provides more accurate energy spectra than the QRM, challenging the view that the JCM is less fundamental in the USC regime.[47] Rather than optimizing the gauge on a case-by-case basis, a more advanced approach is to develop gauge-independent truncation schemes for the light-matter interaction Hamiltonians. Gauge dependence has been attributed to the nonlocalities introduced during the construction of the effective Hamiltonian in the truncated Hilbert space.[48] One method to address this issue involves applying a minimal-coupling replacement to the nonlocal potential while truncating both the atomic Hamiltonian and the gauge transformation operator.[48,49] Another approach consistently substitutes truncated operators in each term of the full Hamiltonian.[50–52] The choice of gauge also influences the definition of QED subsystems, as noted in Ref. [53]; studies on gauge dependence have informed gauge-independent interaction theories, including applications in operational measurements,[54] emission spectra,[55] open systems,[56] arbitrary media,[57] the Dicke model,[58,59] and the Hopfield model.[58] The dependence of the optimal gauge choice on multicavity modes has been linked to specific

*Corresponding author. Email: wlyou@nuaa.edu.cn; lanyh@bupt.edu.cn; mxliu@bnu.edu.cn
© 2025 Chinese Physical Society and IOP Publishing Ltd. All rights, including for text and data mining, AI training, and similar technologies, are reserved.

modes and observables.[60,61] These findings indicate that before fully addressing the issue of gauge dependence, it is crucial to undertake in-depth and specialized research on gauge ambiguity. Here, we analyze various external potentials acting on the atom to quantify the gauge dependence by examining observables, such as ground-state energy, ground-state fidelity, energy spectra, and dynamics.

Quantum Rabi Model in an Arbitrary-Gauge Formalism with a Finite-Level Truncation. The QRM in the arbitrary-gauge formalism with d-level truncation is

$$\begin{aligned} H_{\rm d}^{\alpha} &= \mathscr{P}_{\rm d}^{\alpha} H^{\alpha} \mathscr{P}_{\rm d}^{\alpha} \\ &= \sum_{i=0}^{d-1} \epsilon_i |\epsilon_i^{\alpha}\rangle\langle\epsilon_i^{\alpha}| + \omega_{\alpha}\left(b_{\alpha}^{\dagger} b_{\alpha} + \frac{1}{2}\right) + \frac{\alpha^2 q^2}{2v\varepsilon_0} \sum_{i,j,k=0}^{d-1} r_{i,k} r_{k,j} \\ &\quad - \frac{(1-\alpha)q}{m}\sqrt{\frac{1}{2\omega_{\alpha}}} \sum_{i,j=0}^{d-1} p_{i,j} |\epsilon_i^{\alpha}\rangle\langle\epsilon_j^{\alpha}| \boldsymbol{e}_{\lambda} (b_{\alpha}^{\dagger} + b_{\alpha}) \\ &\quad + \frac{i\alpha q}{\varepsilon_0}\sqrt{\frac{\omega_{\alpha}}{2}} \sum_{i,j=0}^{d-1} r_{i,j} |\epsilon_i^{\alpha}\rangle\langle\epsilon_j^{\alpha}| \boldsymbol{e}_{\lambda} (b_{\alpha}^{\dagger} - b_{\alpha}), \end{aligned} \tag{1}$$

where the projection operator $\mathscr{P}_{\rm d}^{\alpha} = \sum_{i=0}^{d-1} |\epsilon_i^{\alpha}\rangle\langle\epsilon_i^{\alpha}|$ truncates the atomic Hilbert space to the d lowest eigenstates $|\epsilon_i^{\alpha}\rangle$ of the atomic Hamiltonian H_a^{α}, with the corresponding eigenvalues ϵ_i. The first term describes the truncated atomic energy levels, while the second term is the photonic Hamiltonian, where ω_{α} denotes the renormalized photonic frequency and b_{α} ($b_{\alpha}^{\dagger}$) denotes the photon annihilation (creation) operators. The interaction terms involve matrix elements of the atomic position $r_{i,\,j} = \langle\epsilon_i^{\alpha}|\boldsymbol{r}|\epsilon_j^{\alpha}\rangle$ and momentum $p_{i,\,j} = \langle\epsilon_i^{\alpha}|\boldsymbol{p}^{\alpha}|\epsilon_j^{\alpha}\rangle$ operators. Here, α represents the gauge parameter that interpolates between the Coulomb gauge ($\alpha = 0$) and dipolar gauge ($\alpha = 1$), $\boldsymbol{e}_{\lambda}$ represents the polarization vector, q represents the charge, v represents the mode volume, and ε_0 represents the permittivity of free space. Additional details and derivations are provided in the Supplementary Material (SM).[62]

Under finite-level truncation, gauge invariance is broken.[47] Setting $d = 2$ results in the QRM in arbitrary gauge formalism,

$$\begin{aligned} H_2^{\alpha} &= \frac{\Omega}{2}\sigma_z + \omega_{\alpha}\left(b_{\alpha}^{\dagger} b_{\alpha} + \frac{1}{2}\right) + \Delta^{\alpha} \\ &\quad - \frac{(1-\alpha)q}{m}\sqrt{\frac{1}{2\omega_{\alpha}}}\Omega r_{1,0}\sigma_y \boldsymbol{e}_{\lambda}(b_{\alpha}^{\dagger} + b_{\alpha}) \\ &\quad + \frac{i\alpha q}{\varepsilon_0}\sqrt{\frac{\omega_{\alpha}}{2}}\sigma_x r_{1,0}\boldsymbol{e}_{\lambda}(b_{\alpha}^{\dagger} - b_{\alpha}), \end{aligned} \tag{2}$$

where $\Omega = (\epsilon_1 - \varepsilon_0)$ denotes the transition frequency of the atom and $\Delta^{\alpha} = \frac{(\epsilon_1+\varepsilon_0)}{2} + \frac{\alpha^2 q^2}{2v\varepsilon_0}(\mathscr{P}_2^{\alpha}\boldsymbol{r}\mathscr{P}_2^{\alpha})^2$ denotes the energy shift. For a Coulomb gauge with $\alpha = 0$, Eq. (2) restores the widely used standard QRM in most previous studies. Note that the derivation of Eq. (2) has assumed the symmetric potential about the origin, i.e., $\langle\epsilon_i^{\alpha}|\boldsymbol{r}|\epsilon_i^{\alpha}\rangle = 0$, and the resulted Hamiltonian (2) is simplified. The result in Eq. (2) is consistent with the one obtained in Ref. [47]. Furthermore, QRM can conventionally be extended to any finite-level truncation in this framework.

Numerical Results. We then discuss an approach to determine the optimal gauge. First, we analyze the ground-state properties, including the ground-state energy and fidelity. Next, we define the concept of an optimal dynamic gauge using the out-of-time-order correlator (OTOC) as a revealing metric. The optimal gauge was identified by comparing the results obtained from the gauge-dependent Hamiltonian of the QRM in Eq. (2) with the full Hamiltonian H^{α}, which is gauge invariant. For simplicity, we set Ω as the unit energy scale in the following discussion, making the Hamiltonian dimensionless.

To compute the Hamiltonians H^{α} and H_2^{α}, a specific form of potential energy $V(r)$ is required. In this study, we focus on two typical potentials: the square-well potential and the harmonic potential. The square well potential is defined as follows:

$$V(x) = \begin{cases} 0, & -1/2 < x < 1/2, \\ \infty, & \text{elsewhere}, \end{cases} \tag{3}$$

and the harmonic potential is expressed as:

$$V(x) = \frac{1}{2}x^2. \tag{4}$$

To test the generality of these two potential forms, we studied three additional cases: linear, double-well, and quadruple-well potentials. Detailed results can be found in the SM.[62]

First, consider the ground state energy $E_{\rm g}$. As $d \to \infty$, the truncated Hamiltonian $H_{\rm d}^{\alpha}$ in Eq. (1) approaches the full Hamiltonian H^{α}. For a sufficiently large d, H^{α} can be accurately approximated, and the exact ground-state energy is expressed as $E_{{\rm g},\,\infty} = \langle\psi_{\infty}^{\alpha}|H_{\infty}^{\alpha}|\psi_{\infty}^{\alpha}\rangle$, where $|\psi_{\infty}^{\alpha}\rangle$ denotes the ground state of H_{∞}^{α}. For the finite-level QRM, the ground-state energy is $E_{{\rm g},\,{\rm d}}^{\alpha} = \langle\psi_{\rm d}^{\alpha}|H\infty^{\alpha}|\psi_{\rm d}^{\alpha}\rangle$, where $|\psi_{\rm d}^{\alpha}\rangle$ represents the ground state of $H_{\rm d}^{\alpha}$, satisfying $H_{\rm d}^{\alpha}|\psi_{\rm d}^{\alpha}\rangle = E_{{\rm g},\,{\rm d}}^{\alpha}|\psi_d^{\alpha}\rangle$. In this study, we mainly consider a two-level approximation ($d = 2$).

By comparing $E_{{\rm g},\,\infty}$ and $E_{{\rm g},\,2}^{\alpha}$, the optimal gauge $\alpha_{\rm o}$ is identified as the value of α that minimizes the energy difference, $\Delta E_{\rm g}^{\alpha} = E_{{\rm g},\,\infty} - E_{{\rm g},\,2}^{\alpha}$. Figure 1 compares the ground-state energy for the two-level QRM ($d = 2$) and the full Hamiltonian using both the square-well and harmonic potentials. For both potentials, $E_{{\rm g},\,\infty}$ remains gauge-invariant, whereas $E_{{\rm g},\,2}^{\alpha}$ exhibits a gauge dependence. The optimal gauges were found to be $\alpha_{\rm o} = 0.847$ for the square well and $\alpha_{\rm o} = 0.469$ for the harmonic potential, both of which fell between those of the dipole gauge ($\alpha = 1$) and Coulomb gauge ($\alpha = 0$).

To examine the characteristics of the ground-state energy, we analyze how the energy difference $\Delta E_{\rm g}^{\alpha}$ varied with the gauge parameter and cavity frequency. Figure 2 shows a contour map of $\log \Delta E_{\rm g}^{\alpha}$, which reveals that the optimal gauge depends on the cavity frequency. At the limit $\omega/\Omega \to 0$, the optimal gauge approaches the dipole gauge, whereas for $\omega/\Omega \to \infty$, the optimal gauge becomes the Coulomb gauge. Although both potentials showed similar qualitative trends, their quantitative behavior differed. Notably, $\Delta E_{\rm g}^{\alpha}$ is significantly smaller for the square well than for the harmonic potential.

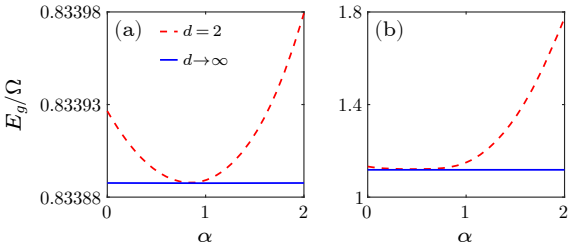

Fig. 1. Comparison of the ground-state energy for the two-level QRM (red dashed lines) and the full Hamiltonian (blue solid lines) at $\omega/\Omega = 1$. (a) For the square-well potential, the optimal gauge is $\alpha_o = 0.847$. (b) For the harmonic potential, the optimal gauge is $\alpha_o = 0.469$.

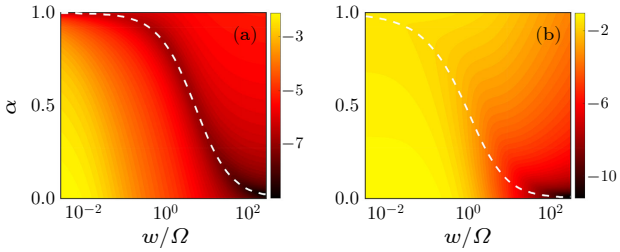

Fig. 2. Contour map of $\log(\Delta E_g^\alpha)$ as a function of α and ω/Ω. The white dashed curves show the optimal gauge minimizing ΔE_g^α for (a) the square-well potential and (b) the harmonic potential. As $\omega/\Omega \to 0$, the optimal gauge approaches $\alpha_o \to 1$ (dipole gauge), and as $\omega/\Omega \to \infty$, it approaches $\alpha_o \to 0$ (Coulomb gauge).

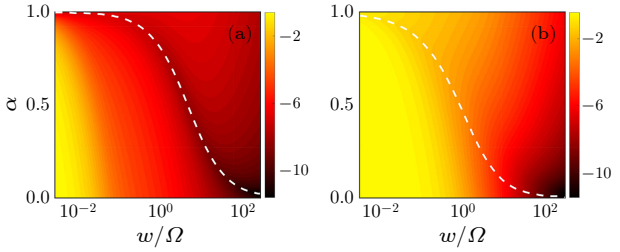

Fig. 3. Contour map of the $\log(1-\mathcal{F}_g^\alpha)$ with respect to α and ω/Ω. Optimal gauge (white dashed line) is determined by finding the minimal value under every ω/Ω, (a) in square-well potential and (b) in harmonic potential. The qualitative similarities and quantitative differences in the asymptotic behaviors of the optimal gauge can be extracted, similar to those determined by the ground state energy.

The ground-state fidelity, defined as $\mathcal{F}_g^\alpha = |\langle\psi_{g,2}^\alpha|\psi_{g,\infty}^\alpha\rangle|^2$, provides an alternative measure to assess the optimal gauge. Figure 3 shows $\log(1-\mathcal{F}_g^\alpha)$ for various values of ω and α. Although there were slight quantitative differences compared to the ground-state energy results, the qualitative asymptotic behavior was consistent across both methods.

The energy spectrum E_n for the first ten levels is an important parameter for the analysis. The optimal gauge for each level was determined in a manner similar to that for the ground-state case. For the square well potential [Fig. 4(a)], the low-energy levels are well reproduced by the two-level QRM; however, significant deviations occur at higher levels. The optimal gauge was close to, but not exactly, $\alpha = 1$ (the dipole gauge). With respect to the harmonic potentials [Fig. 4(b)], the optimal gauge changes notably with increasing energy levels and is neither the Coulomb nor the dipole gauge. The two-level QRM is less accurate with harmonic potential, especially at high levels, where it predicts level degeneracy at certain gauges that do not exist in the full Hamiltonian. Careful gauge selection is crucial for the excited states. Similar to the ground state, the optimal gauge for the excited states can also be assessed using fidelity, showing consistent qualitative results.

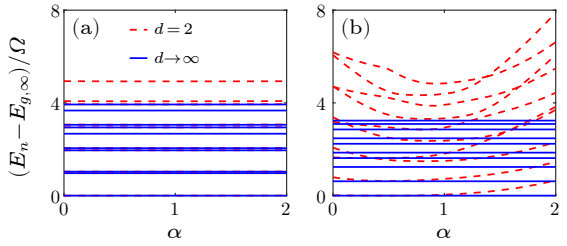

Fig. 4. Energy spectrum comparison for the first ten levels between the two-level QRM and the full Hamiltonian at $\omega/\Omega = 1$. (a) For the square-well potential, the two-level spectrum approximates gauge invariance well for low levels but exhibits gauge dependence, with the optimal gauge differing for each level. (b) For the harmonic potential, the optimal gauges vary significantly across levels, and the two-level QRM predicts additional degeneracies at certain gauges for higher energy levels, which are absent in the full Hamiltonian.

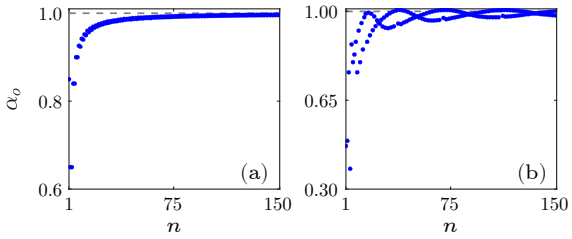

Fig. 5. Optimal gauge behavior as a function of energy level n at $\omega/\Omega = 1$. For $n \to \infty$, the optimal gauge converges to $\alpha = 1$, despite variations at lower levels. Two distinct trajectories are observed, influenced by the two-level truncation of the atomic Hamiltonian. (a) For the square-well potential, the optimal gauge approaches $\alpha = 1$ monotonically. (b) For the harmonic potential, the optimal gauge converges to $\alpha = 1$ with oscillations.

For both square wells [Fig. 5(a)] and harmonic-well [Fig. 5(b)] potentials, the optimal gauge tends to approach the dipole gauge as the energy level increases. This behavior is linked to the localization of the atomic wave function; more localized wave functions favor the Coulomb gauge, whereas less localized ones favor the dipole gauge. In the harmonic potential, the oscillatory behavior of the optimal gauge with energy levels may be related to the intrinsic coherence of the system and warrants further investigation. Although the optimal gauge varies with the energy levels, real-world measurements involve specific energy ranges and a limited number of levels, simplifying the determination of an effective optimal gauge.

Owing to the level of dependence on the optimal gauge,

defining a single metric for the entire spectrum is challenging. However, because the dynamics of the QRM are closely tied to the energy scale of interest, an optimal dynamic gauge can be defined. Consequently, we use the widely studied OTOC, a robust and experimentally accessible metric. OTOC is regarded as a powerful tool for detecting signatures of chaos in quantum systems owing to its early exponential growth. Contrary to classical methods, the OTOC captures quantum dynamical characteristics even in systems without classical counterparts, providing insights into phenomena, such as information scrambling, many-body localization, and phase transitions.[63–67] In QRM, the OTOC is expressed as

$$F^{\alpha}(t) = \langle \psi_{\mathrm{d}}^{\alpha} | W^{\dagger}(t) V^{\dagger}(0) W(t) V(0) | \psi_{\mathrm{d}}^{\alpha} \rangle, \tag{5}$$

where $W = V = b_{\alpha}^{\dagger} b_{\alpha}$ represents the photon number operator and $W(t)$ represents the time evolution under the Hamiltonian H_{∞}^{α}. The photon definition, and consequently, the OTOC, is gauge-dependent. Details of the determination of the optimal dynamical gauge via the mean relative error of the OTOC are provided in the SM.[62]

Figure 6 shows the time evolution of the OTOC for the Coulomb, dipole, and optimal dynamic gauges. The two-level OTOC closely reproduces the full Hamiltonian results in the optimal gauge ($\alpha_{\mathrm{o}} = 0.876$), which is consistent with the findings from the ground-state energy and fidelity. By contrast, as shown in Fig. 7, the two-level OTOC deviates significantly in the Coulomb and dipole gauges but closely matches the full Hamiltonian in the optimal gauge ($\alpha_{\mathrm{o}} = 0.244$), highlighting the importance of an optimal dynamical gauge.

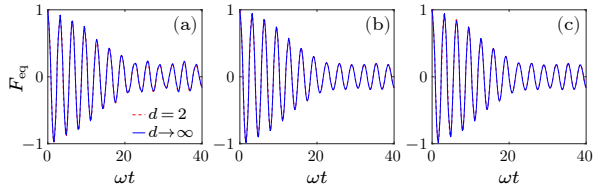

Fig. 6. Time evolution of the OTOC under square well potential (a) in the Coulomb gauge, (b) dipole gauge, and (c) optimal gauge $\alpha_{\mathrm{o}} = 0.876$. The frequency ratio is chosen to be $\omega/\Omega = 1$.

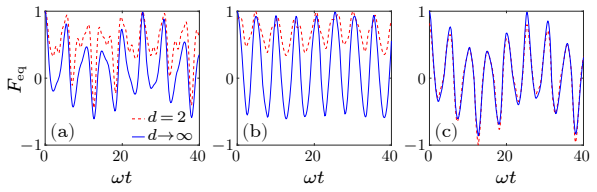

Fig. 7. Time evolution of the OTOC under harmonic potential (a) in the Coulomb gauge, (b) dipole gauge, and (c) optimal gauge $\alpha_{\mathrm{o}} = 0.244$. The frequency ratio is chosen to be $\omega/\Omega = 1$.

Conclusion. In this study, we investigated optimal static and dynamic gauges in the QRM for various potentials. The optimal static gauge was determined by identifying the gauge that minimized the difference between the two-level and accurate ground-state energies and low-energy spectra. We found that the dipole and Coulomb gauges were optimal in the low-frequency and high-frequency limits, respectively, with the dipole gauge being optimal for higher energy levels. For the dynamic gauge, we analyzed the time evolution of the OTOC and determined the optimal gauge by minimizing the mean error between the two levels of accuracy. The dynamic gauges for both potentials differ from their static counterparts, highlighting the importance of introducing optimal dynamic gauges.

Establishing an analytical relationship between the optimal gauge and other influencing factors is crucial for developing a gauge-independent theory in a truncated Hilbert space, which is one of the most important tasks in the field of light–matter interactions. Utilizing the gauge choice, additional symmetries contribute to the construction of accurate approximate theories for practical calculations. The framework employed in our study allows for straightforward extensions to various truncation levels. This will be instrumental in future systematic and analytical studies addressing gauge issues. The optimal gauge considerations extend beyond the QRM and are applied to any system with redundant degrees of freedom in constructing effective theories. In QED systems, the experimental coupling between the field and the atom relative to the cavity frequency falls on the order of 10^{-3}.[68,69] However, because this study was based on a one-dimensional model, direct comparisons with experimental parameters remain subtle and deserve further study.

Acknowledgements. This study was supported by the National Natural Science Foundation of China (Grant Nos. 12174194 and 12475033) and the Fundamental Research Funds for the Central Universities.

References

[1] Cabibbo N, Maiani L, and Benhar O 2017 *An Introduction to Gauge Theories* (CRC Press)
[2] Cohen-Tannoudji C, Dupont-Roc J, and Grynberg G 1997 *Photons and Atoms - Introduction to Quantum Electrodynamics*
[3] Göppert-Mayer M 1931 *Ann. Phys.* **401** 273
[4] Lamb Jr W E 1952 *Phys. Rev.* **85** 259
[5] Power E A and Zienau S 1959 *Philos. Trans. R. Soc. London, Ser. A* **251** 427
[6] Woolley R G 1971 *Proc. R. Soc. London, Ser. A* **321** 557
[7] Bassani F, Forney J J, and Quattropani A 1977 *Phys. Rev. Lett.* **39** 1070
[8] Forney J J, Quattropani A, and Bassani F 1977 *Il Nuovo Cimento B* **37** 78
[9] Kobe D H and Smirl A L 1978 *Am. J. Phys.* **46** 624
[10] Kobe D H 1978 *Phys. Rev. Lett.* **40** 538
[11] Yang K H 1982 *Phys. Lett. A* **92** 71
[12] Lamb Jr W E, Schlicher R R, and Scully M O 1987 *Phys. Rev. A* **36** 2763
[13] Woolley R G 2000 *Proc. R. Soc. London, Ser. A* **456** 1803
[14] Rzążewski K and Boyd R W 2004 *J. Mod. Opt.* **51** 1137
[15] Rabi I I 1936 *Phys. Rev.* **49** 324
[16] Rabi I I 1937 *Phys. Rev.* **51** 652
[17] Reiserer A 2022 *Rev. Mod. Phys.* **94** 041003
[18] Román-Roche J, and Zueco D 2022 *SciPost Phys. Lect. Notes* 50

[19] Casanova J, Romero G, Lizuain I *et al.* 2010 *Phys. Rev. Lett.* **105** 263603
[20] Yoshihara F, Fuse T, Ashhab S *et al.* 2017 *Nat. Phys.* **13** 44
[21] Yoshihara F, Fuse T, Ao Z *et al.* 2018 *Phys. Rev. Lett.* **120** 183601
[22] Mueller N S, Okamura Y, Vieira B G M *et al.* 2020 *Nature* **583** 780
[23] Yoshihara F, Ashhab S, Fuse T, Bamba M, and Semba K 2022 *Sci. Rep.* **12** 6764
[24] De Liberato S 2014 *Phys. Rev. Lett.* **112** 016401
[25] Le Boité A, Hwang M J, Nha H, and Plenio M B 2016 *Phys. Rev. A* **94** 033827
[26] Stassi R, Macrì V, Kockum A F *et al.* 2017 *Phys. Rev. A* **96** 023818
[27] De Bernardis D 2023 *Phys. Rev. A* **108** 043717
[28] Romero G, Ballester D, Wang Y M, Scarani V, and Solano E 2012 *Phys. Rev. Lett.* **108** 120501
[29] Stassi R and Nori F 2018 *Phys. Rev. A* **97** 033823
[30] Macrì V, Nori F, and Kockum A F 2018 *Phys. Rev. A* **98** 062327
[31] Forn-Díaz P, Lamata L, Rico E, Kono J, and Solano E 2019 *Rev. Mod. Phys.* **91** 025005
[32] Stassi R, Cirio M, and Nori F 2020 *npj Quantum Inf.* **6** 67
[33] Hepp K and Lieb E H 1973 *Ann. Phys.* **76** 360
[34] Rzażewski K, Wódkiewicz K, and Żakowicz W 1975 *Phys. Rev. Lett.* **35** 432
[35] Hwang M J, Puebla R, and Plenio M B 2015 *Phys. Rev. Lett.* **115** 180404
[36] Hwang M J and Plenio M B 2016 *Phys. Rev. Lett.* **117** 123602
[37] Liu M X, Chesi S, Ying Z J *et al.* 2017 *Phys. Rev. Lett.* **119** 220601
[38] Guerci D, Simon P, and Mora C 2020 *Phys. Rev. Lett.* **125** 257604
[39] Ashhab S 2013 *Phys. Rev. A* **87** 013826
[40] Chen X, Wu Z, Jiang M, Lü X Y, Peng X H, and Du J F 2021 *Nat. Commun.* **12** 6281
[41] Zheng R H, Ning W, Chen Y H *et al.* 2023 *Phys. Rev. Lett.* **131** 113601
[42] Braak D 2011 *Phys. Rev. Lett.* **107** 100401
[43] Larson J 2013 *J. Phys. B: At. Mol. Opt. Phys.* **46** 224016
[44] He S, Duan L W, and Chen Q H 2015 *New J. Phys.* **17** 043033
[45] Grimaudo R, Magalhães de Castro A S, Messina A, Solano E, and Valenti D 2023 *Phys. Rev. Lett.* **130** 043602
[46] De Bernardis D, Pilar P, Jaako T, De Liberato S, and Rabl P 2018 *Phys. Rev. A* **98** 053819
[47] Stokes A and Nazir A 2019 *Nat. Commun.* **10** 499
[48] Di Stefano O, Settineri A, Macrì V, Garziano L, Stassi R, Savasta S, and Nori F 2019 *Nat. Phys.* **15** 803
[49] Savasta S, Di Stefano O, Settineri A, Zueco D, and Hughes S 2021 *Phys. Rev. A* **103** 053703
[50] Taylor M A D, Mandal A, Zhou W, and Huo P 2020 *Phys. Rev. Lett.* **125** 123602
[51] Taylor M A D, Mandal A, and Huo P 2022 *Opt. Lett.* **47** 1446
[52] Ryu C J, Na D Y, and Chew W C 2023 *Phys. Rev. A* **107** 063707
[53] Stokes A and Nazir A 2022 *Rev. Mod. Phys.* **94** 045003
[54] Settineri A, Di Stefano O, Zueco D, Hughes S, Savasta S, and Nori F 2021 *Phys. Rev. Res.* **3** 023079
[55] Mercurio A, Macrì V, Gustin C, Hughes S, Savasta S, and Nori F 2022 *Phys. Rev. Res.* **4** 023048
[56] Salmon W, Gustin C, Settineri A, Di Stefano O, Zueco D, Savasta S, Nori F, and Hughes S 2022 *Nanophotonics* **11** 1573
[57] Gustin C, Franke S, and Hughes S 2023 *Phys. Rev. A* **107** 013722
[58] Garziano L, Settineri A, Di Stefano O, Savasta S, and Nori F 2020 *Phys. Rev. A* **102** 023718
[59] Akbari K, Salmon W, Nori F, and Hughes S 2023 *Phys. Rev. Res.* **5** 033002
[60] Roth M, Hassler F, and DiVincenzo D P 2019 *Phys. Rev. Res.* **1** 033128
[61] Arwas G, Manucharyan V E, and Ciuti C 2023 *Phys. Rev. A* **108** 023714
[62] See Supplemental Materials for more details, including (I) the detail of deriving the quantum rabi model in an arbitrarygauge formalism with a finite-level truncation, (II) identification of the longitudinal component of the vector potential in reciprocal space, (III) numerical results in other potentials, (IV) gauge dependence of the mean error of the OTOC, (V) gauge dependence for higher-level approximation, and (VI) implications of energy scale choice in the OTOC.
[63] Rozenbaum E B, Ganeshan S, and Galitski V 2017 *Phys. Rev. Lett.* **118** 086801
[64] Shen H, Zhang P, Fan R, and Zhai H 2017 *Phys. Rev. B* **96** 054503
[65] Swingle B 2018 *Nat. Phys.* **14** 988
[66] Sun Z H, Cai J Q, Tang Q C, Hu Y, and Fan H 2020 *Ann. Phys.* **532** 1900270
[67] Kirkova A V, Porras D, and Ivanov P A 2022 *Phys. Rev. A* **105** 032444
[68] Raimond J M, Brune M, and Haroche S 2001 *Rev. Mod. Phys.* **73** 565
[69] Walther H, Varcoe B T H, Englert B G, and Becker T 2006 *Rep. Prog. Phys.* **69** 1325